Evaluation of Radiographically Evident Cardio-Pulmonary, Metastatic and Paraneoplastic Changes in Thorax Associated with Superficial and Mammary Neoplasms in Dogs

By Lekshmi S.L, Sudheesh S Nair, Sajitha I.S, Narayanan M.K. & K.D. John Martin

Kerala Veterinary and Animal Sciences University

Abstract- Nowadays, neoplasms have become the common surgical affections encountered in the pet population, especially in dogs. Skin neoplasms are the most common neoplasm observed in dogs, followed by mammary neoplasms. Most of the neoplasm may exhibit metastatic and paraneoplastic changes in distant sites other than primary tumor sites, mainly in the thorax. The present study investigated the evaluation of radiographically evident cardio-pulmonary, metastatic and paraneoplastic changes in the thorax of twenty- four clinical cases of dogs of either sex belonging to different breeds, and age, having superficial cutaneous and mammary neoplasm conditions.

Keywords: pulmonary metastasis, computed thoracic radiography, atypical metastatic lesions.

GJMR-G Classification: DDC Code: 818.540308036 LCC Code: SF416

EVALUATIONOFRADIOGRAPHICALLYEVIDENTCARDIOPULMONARYMETASTATICANDPARANEOPLASTICCHANGESINTHORAXASSOCIATEDWITHSUPERFICIALANDMAMMARYNEOPLASMSINDOGS

Strictly as per the compliance and regulations of:

Evaluation of Radiographically Evident Cardio-Pulmonary, Metastatic and Paraneoplastic Changes in Thorax Associated with Superficial and Mammary Neoplasms in Dogs

Lekshmi S.L [α], Sudheesh S Nair [σ], Sajitha I.S [ρ], Narayanan M.K. [ω] & K.D. John Martin [¥]

Abstract- Nowadays, neoplasms have become the common surgical affections encountered in the pet population, especially in dogs. Skin neoplasms are the most common neoplasm observed in dogs, followed by mammary neoplasms. Most of the neoplasm may exhibit metastatic and paraneoplastic changes in distant sites other than primary tumor sites, mainly in the thorax. The present study investigated the evaluation of radiographically evident cardio-pulmonary, metastatic and paraneoplastic changes in the thorax of twenty-four clinical cases of dogs of either sex belonging to different breeds, and age, having superficial cutaneous and mammary neoplasm conditions. Fine Needle Aspiration Cytology (FNAC) of the primary tumour was performed on all of the dogs for neoplasm confirmation, and orthogonal thoracic radiography was used to assess each region of the thorax, including the pleura, pulmonary parenchyma, mediastinum, trachea, cardiovascular system, and extrathoracic structures. The size, morphology, and area of distribution of metastatic pulmonary lesions, as well as atypical metastatic lesions such as calcification, secondary pneumothorax, feeding vessel signs, cavitation, were assessed in three-view thoracic radiographs of both neoplasm conditions, and the results are described here.

Keywords: pulmonary metastasis, computed thoracic radiography, atypical metastatic lesions.

I. Introduction

Radiographic examination is usually considered as the first investigative modality, after the clinical examination and undisputedly most beneficial, being non-invasive which can provide rapid and valuable information in the diagnosis and treatment of a wide range of diseases (Rudorf *et al.,* 2008). Radiography remains a popular diagnostic screening tool for the thorax because it is time- and cost-efficient, uses readily available equipment, is relatively easy to perform, usually does not require general anesthesia, is non-invasive, and causes relatively low stress to the patient, and is unrivalled by any other diagnostic test for these characteristics. The main advantage over other more recent techniques is the inherent revelation of the morphology of thoracic structures. Most neoplasms metastasize to the lung, particularly mammary neoplasms, with solitary or numerous pulmonary nodules, either benign or malignant, lymphangitic metastasis, and/or endobronchial metastasis being common lesions (Jung *et al*., 2004). An awareness of the spectrum of radiology for indications in pulmonary metastases and pulmonary changes in paraneoplastic syndrome allows the distinction of metastases from other non-malignant pulmonary diseases. The evaluation of radiographically evident cardio- pulmonary, metastatic, and paraneoplastic chnages in the thorax of twenty-four clinical cases of superficial and mammary neoplasms in dogs is documented in this work.

II. Materials and Methods

The selected animals were grouped into two containing twelve animals each – group I with superficial neoplasm designated as A1 to A12 and group II with mammary neoplasm as B1 to B12. Fine Needle Aspiration Cytology (FNAC) of primary tumor mass was carried out in all dogs to confirm the malignancy before the imaging examination. A 200 mA X-ray machine with a computed radiography system was used to perform a three-way thoracic radiographic evaluation (right lateral, left lateral, and ventrodorsal views) on all cases. All animals were subjected to surgical management, and excisional biopsy of tumor samples were histopathologically analysed.

Tracheal Diameter: Tracheal Inlet (TD: TI) ratio was calculated by recording the diameter of the trachea at the level of the thoracic inlet and the inner diameter of the thoracic inlet (Fig 1). Cardiothoracic ratios (CTR) were calculated by dividing the largest width of the thorax by chest depth on radiographs (Fig 3). On a dorsoventral/ventrodorsal radiograph, the width of the thorax was measured as the distance between the medial borders of the eight ribs (Fig 4). The depth was

Corresponding Author α: M.V.Sc. scholar, Department of Veterinary Surgery and Radiology, College of Veterinary and Animal Sciences, Mannuthy, 680651, Kerala, India. e-mail: lekshmi25krishna@gmail.com
Author σ: Assistant Professor, Department of Veterinary Surgery and Radiology.
Author ρ: Assistant Professor, Department of Veterinary Pathology.
Author ω: Professor, Department of Veterinary Surgery and Radiology.
Author ¥: Professor and Head, Department of Veterinary Surgery and Radiology.

assessed on the right lateral radiographic view from the dorsal margin of the xiphoid process to the ventral margin of the vertebral body, with the electronic calipers aligned perpendicular to the vertebral column. The Vertebral heart score was calculated according to Buchanan and Bücheler, 1995 (Fig 2).

Radiographical assessment of each region of thorax, including pleura, pulmonary parenchyma, cardiac silhouette, mediastinum and trachea, as well as extrathoracic structures, including sternum, ribs, vertebrae, thoracic wall, and diaphragm were performed.

The primary lesions studied were pleural effusion, pleural mass and change in radiodensity for pleura and pulmonary patterns (bronchial, interstitial, alveolar, vascular, and mixed pattern) and other pulmonary parenchymal lesions (peribronchial thickening, bronchial mineralization, lobar signs, consolidation, cavitary lesions, generalized increased lung opacity, and pneumothorax) for lung parenchyma. The presence of mediastinal masses and pneumomediastinum, as well as other radiographic aspects of the mediastinum, were investigated. Tracheal changes, such as tracheal mineralization, tracheal deviation, tracheal hypoplasia, etc., were also evaluated.

The cardiac silhouette features observed in orthogonal thoracic radiographs were categorized as positional shift, chamber enlargement (left and right atrial enlargement, left and right ventricular enlargement), pericardial effusion, and pulmonary arterial or venous changes.

The extrathoracic region including, sternum (sternal spondylosis and degenerative changes), ribs (costal cartilage mineralization, degenerative changes, and other lesions), vertebrae (vertebral spondylosis and intervertebral herniation), thoracic wall changes, and diaphragmatic abnormalities were all investigated.

This study also investigated at the size, morphology, and distribution area of pulmonary metastatic lesions as well as the atypical metastatic lesions such as calcification, secondary pneumothorax, feeding vessel signs, cavitation lesions, and so on.

III. Results and Discussion

All the cases were confirmed as neoplasm by performing Fine Needle Aspiration Cytology (FNAC) of the primary tumor. The cytology of superficial neoplasms revealed two (16.67 percent) mesenchymal tumors, five (55.55 percent) epithelial tumors and, one (11.11 percent) round cell tumors (A3). Four (33.33 percent) out of 12 samples were classified as inadequate for diagnosis because of no cells (n =2) and the presence of a large number of red blood cells and inflammatory cells (n=2). The malignancy was indicated by the presence of clusters of cells with anisocytosis,

anisokaryosis, and hyperchromasia, as well as nuclear anomalies such as the double nucleus, giant nucleus, mitotic figures, and abnormal chromatin structures. Similar observations were also reported by Meinkoth *et al.* (2007), Yildirim and Gurel (2012), and Yumusak and Kutsal (2016). In mammary neoplasms, the common cytological characteristics observed were anisocytosis, anisokaryosis, enlarged nuclei, double nuclei, multiple nucleoli, and clumping of chromatin (hyperchromasia). These findings were as per Shafiee *et al.* (2013) and Kuppusamy *et al.* (2019).

Tracheal diameter: Thoracic inlet ratios was calculated from lateral radiographs in all animals by the method proposed by Harvey and Fink (1982). Three of the animals with mammary neoplasm had a ratio of less than 0.2, indicating tracheal hypoplasia, whereas the TD: TI ratio in superficial neoplasm affected animals was in the normal range, indicating normal tracheal confirmation. The relationship between TD: TI ratio and neoplasm conditions was not yet reported. The finding of tracheal hypoplasia in this study could be related to other physiological factors. The exact measurements of the tracheal diameter were challenging with radiography owing to the absence of sharp luminal borders due to overlying soft tissues as opined by Fingland *et al.* (1995).

From measurements of Vertebral Heart Score in both right lateral and left lateral thoracic radiographs, 33.33 percent of group I animals and 25 percent of group II animals were diagnosed as suffering from cardiomegaly. There was no significant difference between the groups. A VHS over 10.7 on the lateral radiograph was a moderately accurate sign of cardiac disease, as opined by Lamb *et al.* (2000). The highest vertebral heart score in the dogs might be due to the onset of mitral valve regurgitation following congestive heart failure, as documented by Lord (2010). The pulmonary metastases of malignancy might be lead to epicardial, myocardial and, endocardial involvement and further pathophysiological changes such as pericardial effusion, filling impairment, myocardial dysfunction, etc., as documented by Bussani *et al.* (2007).

Group I animals had a Cardio-thoracic ratio ranging from 0.73- 1.03, and Group II had a cardio-thoracic ratio ranging from 0.69-1.12. All the animals had CTR values in the normal range irrespective of type of the neoplasm.

Pleura was identified as very thin and silhouetted with adjacent soft tissue everywhere except in interlobar fissures, where it was in contact only with the lung. In the present study, normal pleura was not visible radiographically, but the pathology of pleura enhanced the radiographic diagnostic visibility as documented by Thrall (2018). Pleural effusion, change in radiodensity, and extrapleural lesions were the most

common radiographically visible pleural lesions observed in this study. Pleural effusion was observed in lateral thoracic radiographs of two cases of mammary neoplasm and four cases of superficial neoplasm. There was no significant difference in pleural lesions between the superficial and mammary neoplasm conditions. The most common cause of pleural effusion was identified as pleural metastasis by Noone (1985).

The typical pulmonary pattern observed in both superficial and mammary neoplasm conditions were interstitial nodular pattern followed by bronchial pattern, alveolar pattern, and vascular pattern. Similar pulmonary patterns were observed by Gupta *et al.* (2014) in thoracic radiograph of dogs affected with mammary neoplasm, which showed a nodular pattern, miliary pattern, alveolar pattern, doughnut pattern and mixed interstitial and bronchial pattern evident in most of the animals. Other pulmonary lesions such as bronchial mineralization, peribronchial thickening, consolidation, lobar symptoms, and pneumothorax were seen in both neoplasm groups with no significant differences.

Many of the mediastinal reflections can be appreciated at conventional radiography, and their presence or distortion could serve as a key to the interpretation of mediastinal abnormalities (Whitten *et al.* 2007). However, computed tomography is the most essential tool in evaluating the mediastinal masses (Takahashi and Al-Janabi, 2010). A mediastinal shift was observed in ventrodorsal radiographs of one animal having superficial neoplasm and two animals having mammary neoplasm. Mediastinal shift, cranioventral mediastinal mass, dorsal mediastinal mass, hilar mediastinal mass, caudoventral mediastinal mass, and pneumomediastinum were seen in both groups of neoplasms in this investigation. There was no significant differences observed between the groups.

The cranioventral aspect of the thorax was one of the most common locations for a mediastinal mass. In this study, cranioventral mass suspecting sternal lymphadenopathy was observed in two cases (A8 and A11) affected with squamous cell carcinoma (Fig 5), one case with liposarcoma (A7), one case with fibroma (A2), and two cases (B1 and B2) with mammary carcinoma . Similar observations were made by Baumann *et al.* (2004) during their study in metastatic disease of dogs affected with mammary gland tumors. Enlarged sternal lymph nodes may result from diseases of the peritoneum, the cranial abdominal organs, or the abdominal orthoracic wall.

The mammary gland complexes I, II, and III usually drain to the axillary lymph nodes and metastasize into the lungs with or without concurrent involvement of the intrathoracic lymph nodes (Brodey *et al.*, 1983 and Pereira *et al.*, 2003). Epithelial tumors, such ascarcinoma, readily metastasize via lymphatics to the regional lymph nodes (Sorenmo, 2003). Hopper *et*

al. (2004) assumed that the sternal lymph node enlargement could be a sign of intrathoracic disease, but enlargement of the sternal lymph node is often secondary to abdominal diseases, such as peritonitis or peritoneal tumor seeding. We assume the cranial mediastinal lymphadenopathy or sternal lymphnode enlargement in these cases is due to metastatic disease. In the present study, pneumomediastinum was observed in two cases from both groups (A9 and B6). Park *et al.* (2003) opined that the pneumomediastinum was a part of the disease process, rather than a complication of pneumothorax, and the most likely cause of the pneumomediastinum found in their patient suffering from angiosarcoma would be cystic rupture into the interstitial space with subsequent tracking of air through the peribronchial space into the mediastinum.

The common radiographical features of the trachea observed in dogs with superficial and mammary neoplasms were mineralization of tracheal rings, tracheal displacement, and tracheal hypoplasia. There was no significant difference observed between these two groups. Similar observations were made by Gowthami (2017) in their study on geriatric dogs. The most commonly observed tracheal displacement in this study was dorsal deviation, which could be due to cranial mediastinal mass, neck positioning during radiography (at craniomediastinal region) or heart base mass, pulmonary artery enlargement, or right atrial enlargement (at heart base), or left atrial enlargement, tracheobronchial lymphadenomegaly or generalized cardiomegaly (at carina) (Thrall, 2013) (Fig 5).

The most common cardiac silhouette changes in this study were left atrial enlargement, left ventricle enlargement, right ventricle enlargement and pericardial effusion in both groups. There is no significant difference noticed between the groups. Tumors could spread to the heart by alternative pathways such as by direct extension, through the bloodstream, through the lymphatic system, and by intracavitary diffusion through either the inferior vena cava or the pulmonary veins (Virmani, 1995). This might lead to epicardial, myocardial, and endocardial involvement and further pathophysiological changes such as pericardial effusion, filling impairment, myocardial dysfunction etc., in humans (Bussani *et al.* 2007). When comparing dogs with mammary neoplasms to dogs with superficial neoplasms, pericardial effusion was found at a higher percentage. In the present study, peripheral artery and vein alterations were observed in lateral radiographs of both groups, more in mammary neoplasm condition.

The common extrathoracic lesions observed in this study were costal cartilage mineralization and degenerative changes in ribs, vertebral spondylosis, and change in opacity of thoracic wall, and presence of soft tissue tumors in the thoracic wall, which mainly observed in the group with superficial neoplasm. Other lesions

such as sternal spondylosis, sternal degenerative changes, diaphragmatic changes (change in position or shape) etc., were also observed in both groups. There is no significant difference noticed between these groups. Exostosis of the ribs (costal cartilage mineralization or calcification) and degenerative or lytic lesions were the prominent lesions observed in ribs of both groups, especially from lateral radiographs. This could be due to age-related changes or the spread of metastatic disease. Schiavon *et al.* (1993) observed that costal cartilage calcification was a common finding in old age, seen as small islands of compact bone tissue or as nodules, mistaken for solitary pulmonary nodules Plasma cell tumors, as well as metastatic dissemination, can cause lytic or proliferative rib changes in felines, according to Adams et al. (2010). Larson (2020) also observed that the aggressive rib changes were metastatic lesions secondary to a diffuse pulmonary carcinoma with secondary pleural effusion.

Depending on the source and type of tumor, the pulmonary metastases could develop a wide range of radiographic appearance (Franquet *et al.* 2020). Pulmonary metastases typically appeared as peripheral, rounded nodules of variable size, scattered throughout both lungs and diffuse thickening of interstitium as per Seo *et al.* (2001). In this study, the categorization of the metastatic lesions noticed in the thoracic radiographs of the neoplasm-affected dogs were performed based on the size of metastatic lesions and distribution pattern or area. Based on the size of metastatic lesions, they were classified into military nodules (<2 mm), pulmonary micronodules (2-7 mm), pulmonary nodules (7- 30mm), and pulmonary mass (>30mm) as per Weerakkody et al. (2019). The most commonly observed pulmonary metastatic lesions were pulmonary nodules followed by pulmonary micronodules, miliary nodules, and pulmonary mass in both groups in lateral thoracic radiographs. The most common pulmonary metastatic nodular pattern in the case of superficial neoplasm cases were pulmonary micronodules and reticulonodular patterns (Fig 7 and Fig 8). Lung consolidation might lead to the formation of pulmonary masses (> 30 mm size), which were observed in both mammary neoplasm and superficial neoplasm in the present study (Fig 6). The similar unusual form of metastatic spread to the lung is characterized by lepidic growth of the tumor cells along the lining of the alveolar walls, resulting in a primary pulmonary adenocarcinoma-like appearance (Franquet *et al*. 2020). Most of the metastatic malignant nodules appeared as lobulated or with spiculations, as observed by Woodring (1990). The radiographic appearance of metastases from benign tumors included multiple peripherally located round variable-sized nodules and tended to remain stable and show prolonged growth (Franquet *et al*. 2020). In the present study, most of the metastatic lesions were located in the perihilar region, followed by the caudodorsal, midventral, and cranioventral area, and in maximum number of cases metastatic lesions were observed uniformly in all lung regions as reported by Gowthami (2017). Other metastatic lesions patterns, such as interstitial disseminated reticulonodular pattern and mixed disseminated alveolar interstitial pattern was observed in both groups. The atypical metastatic lesions such as calcification, secondary pneumothorax, cavitation signs, and feeding vessel signs were observed in this study. Calcification of a pulmonary nodule is usually suggestive of its benign nature but it can also occur in metastatic nodules from an osteosarcoma or chondrosarcoma (Seo *et al*. 2001). Pneumothorax was observed in three mammary neoplasms and one superficial neoplasm case in this study. Weerakkody and Niknejad (2019) reported a "feeding vessel sign," which consisted of a particular vessel leading directly to a nodule or a mass. Some of the malignant metastatic lesions in this study suspected this sign and can be confirmed by computed tomography.
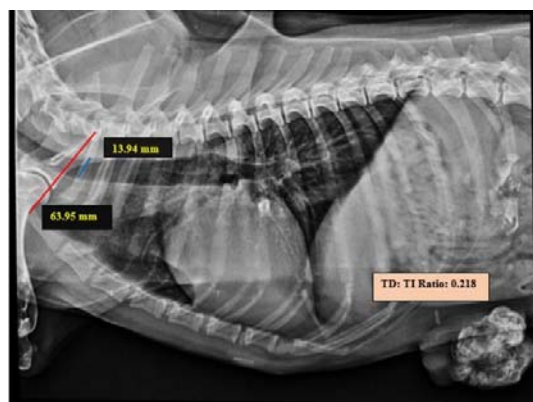

Fig.1: Skiagram showing measurement of TD: TI ratio from the right lateral view
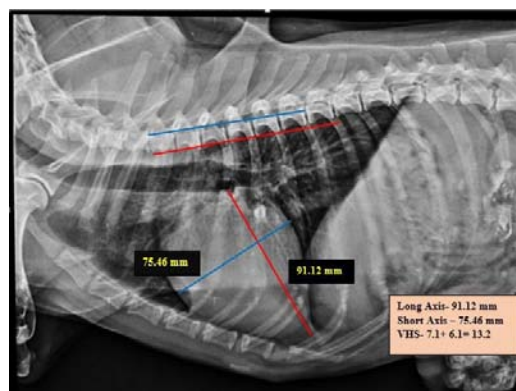

Fig. 2: Skiagram showing measurement of vertebral heart score from the right lateral view
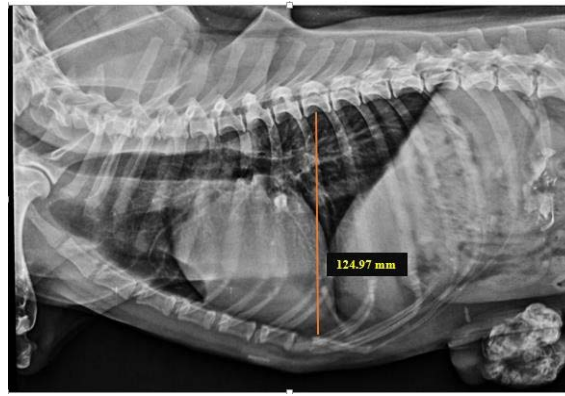
Fig. 3: Skiagram showing measurement of chest depth on right lateral view for assessment of the cardiothoracic ratio
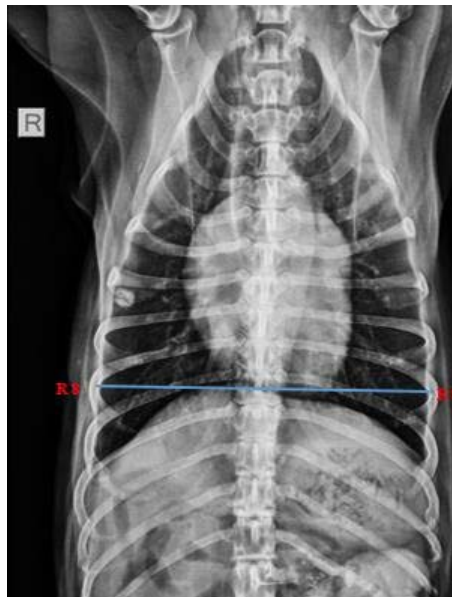

Fig. 4: Skiagram showing measurement of thoracic width on ventrodorsal view for assessment of the cardiothoracic ratio

Cardiothoracic ratio, CTR =
Largest width of the thorax / Chest
Depth = 0.89

Fig. 5: Skiagram of the thorax on the right lateral view showing cranioventral mediastinal mass (1), tracheal displacement (2), and suspecting tracheobronchial lymphadenopathy (3) in dog A11
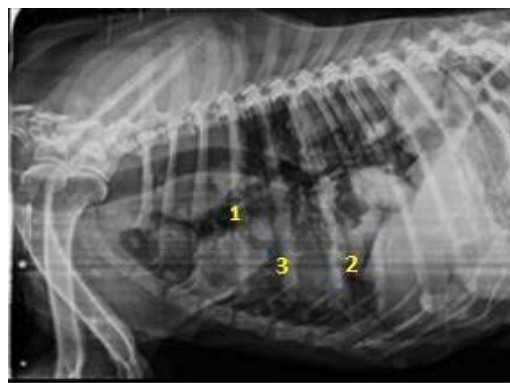

Fig. 6: Skiagram of the thorax on the right lateral view showing cavitary lesion (1), lobar signs (2), consolidation (3), and pulmonary metastatic lesions in dog B11
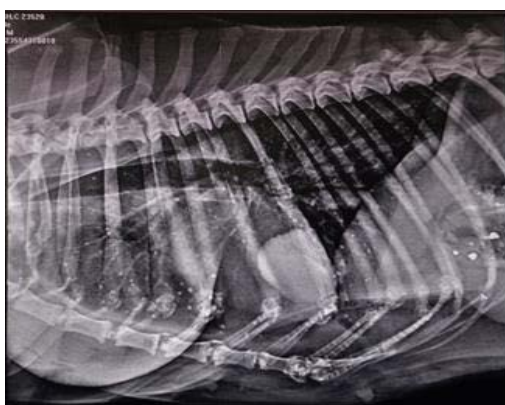

Fig. 7: Skiagram of the thorax showing pulmonary miliary nodules, pulmonary micronodules at the cranioventral region and pulmonary mass at caudoventral region of lung parenchyma and suspecting cavitation at the cranioventral area in right lateral view in dog A9

Fig. 8: Skiagrams of thorax showing Pulmonary mass (Size 34.21mm) at the midventral area and nodular lesion at the caudoventral area and suspecting feeding vessel sign in right lateral view in dog B1

IV. CONCLUSION

Thoracic radiography was found to be a reliable, cost and time-effective diagnostic procedure for the identification of initial or advanced stages of pulmonary metastasis and other paraneoplastic changes associated with neoplasm conditions such as superficial and mammary neoplasms. Even though thoracic radiography is the primary diagnostic choice for pulmonary metastasis, there are so many limitations for using this as a confirmatory diagnosis, such as soft tissue nodules of diameter less than 2mm could not be diagnosed by using radiography. Feeding vessel signs, cavitation, tumor embolism and hemorrhage around the nodule, etc., can be interpreted by other techniques such as CT or MRI.

REFERENCES RÉFÉRENCES REFERENCIAS

1. Adams, C., Streeter, E.M., King, R. and Rozanski, E. 2010. Retrospective Study: Cause and clinical characteristics of rib fractures in cats: 33 cases (2000–2009). *J. Vet. Emerg. Crit. Care*. *20* (4): 436-440.
2. Baumann, D., Hauser, B., Hubler, M. and Flückiger, M. 2004. Signs of metastatic disease on thoracic radiographs of dogs suffering from mammary gland tumours: a retrospective study (1990–1998). *Schweiz. Arch. Tierheilkd. 14:* 431-435.
3. Brodey, R.S. 1983. Canine mammary gland neoplasms. *J. Am. Anim. Hosp. Assoc.19*: 61-90.
4. Buchanan, J.W. and Bucheler, J. 1995. Vertebral scale system to measure canine heart size in radiographs. *J. Am. Vet. Med. Assoc*. *206*: 194-199.
5. Bussani, R., De-Giorgio, F., Abbate, A. and Silvestri, F. 2007. Cardiac metastases. *J. Clin. Pathol*. *60*: 27-34.
6. Fingland, R.B., Layton, C.I., Kennedy, G.A. and Galland, J.C. 1995. A comparison of simple continuous versus simple interrupted suture patterns for tracheal anastomosis after large-

segment tracheal resection in dogs. *Vet. Surg.* 24: 320–330.

7. Franquet, T., Rosado-de-Christenson, M.L., Marchiori, E., Abbott, G.F., Martínez-Jiménez, S.and López, L. 2020. Uncommon thoracic manifestations from extrapulmonary tumors: Computed tomography evaluation-Pictorial review. *Respir. Med.* 20: 105-986.

8. Gowthami, N.G.V. 2017. Computerized radiographic studies of thorax in geriatric dogs. *M.V.Sc. thesis*, Sri Venkateswara Veterinary University, Thirupati, 148p.

9. Gupta, P., Raghunath, M., Gupta, A.K., Sharma, A. and Kour, K. 2014. Clinical study for diagnosis and treatment of canine mammary neoplasms (CMNs) using different modalities. *Indian J. Anim. Res.* 48(1): 45-49.

10. Harvey, C.E. and Fink, E.A. 1982. Tracheal diameter: Analysis of radiographic measurements in brachycephalic and non-brachycephalic dogs. *J. Am. Anim. Hosp. Assoc. 18*: 570- 576.

11. Hopper, B., Lester N. and Irwin P. 2004. Imaging diagnosis: pneumothorax and focal peritonitis in a dog due to migration of an inhaled grass awn. *Vet. Radiol. Ultrasound. 45*(2):136–138.

12. Kuppusamy, K., Rajan, A., Warrier, A., Nadhan, R., Patra, D. and Srinivas, P. 2019. Cytological Grading of Breast Tumors—The Human and Canine Perspective. *Front. Vet. Sci. 6*: 283.

13. Lamb, C.R., Tyler, M., Boswood, A., Skelly B.J. and Cain, M. 2000. Assessment of the value of the vertebral heart scale in the radiographic diagnosis of cardiac disease in dogs. *Vet.Rec. 146* (24): 687-690.

14. Larson, M.M., 2020. Thoracic Cavity. In: Holland, M. and Hudson, J. (eds.), *Feline Diagnostic Imaging*. Wiley-Blackwell, pp. 281-286.

15. Lord, P., Hansson, K. and Kvart, C. 2010. Rate of change of heart size before congestive heart failure in dogs with mitral regurgitation. *J. Small Anim. Pract. 51*: 210–218.

16. Meinkoth, J.H., Cowell, R.H. and Tyler, R.D. 2007. Cell Types and Criteria of Malignancy. C.In: Cowell, R.L., Tyler, R.D., Meinkoth, J.H. and DeNicola, D.B. (eds*.), Diagnostic Cytology and Hematology of the Dog and Cat*. Mosby Elsevier, pp. 37-46.

17. Noone, K.E. 1985. Pleural effusions and diseases of the pleura. *Vet. Clin. North Am. Small Anim. Pract.15*: 1069-1084.

18. Park, S.I., Choi, E., Lee, H.B., Rhee, Y.K., Chung, M.J. and Lee, Y.C. 2003. Spontaneous pneumome-diastinum and hemopneumothoraces secondary to cystic lung metastasis. *Respiration. 70:* 211-213.

19. Pereira, C.T., Rahal, S.C., DeCarvalho Balieiro, J.C. and Ribeiro, A.A. 2003. Lymphatic Drainage on Healthy and Neoplastic Mammary Glands in Female Dogs: Can It Be Really Altered? *Anatomy Histology and Embryology. 32:* 282-290.

20. Schiavon, F., Nardini, S., Favat, M., Manfrin, P. and Chioatto, P. 1993. Radiology of normal chest structures in the elderly patients. *Radiol. Med. 86*: 418-31.

21. Seo, J.B., Im, J.G., Goo, J.M., Chung, M.J. and Kim, M.Y. 2001. Atypical pulmonary metastases: spectrum of radiologic findings. *Radiographics. 21*(2): 403-417.

22. Shafiee, R., Javanbakht, J., Atyabi, N., Bahrami, A., Kheradmand, D., Safaei, R., Khadivar, F. and Hosseini, E. 2013. Comparative value of clinical, cytological, and histopathological features in feline mammary gland tumors; an experimental model for the study of human breast cancer. *Diagn. Pathol. 8*(1): 1-8.

23. Sorenmo, K. 2003. Canine mammary gland tumors. *Vet. Clin. North Am. Small Anim. Pract.* 33(3): 573-596.

24. Takahashi, K. and Al-Janabi, N.J. 2010. Computed tomography and magnetic resonance imaging of mediastinal tumors. *J. Magn. Reson. Imaging. 32*: 1325–1339.

25. Thrall, D. E. 2013. *Text book of veterinary diagnostic radiology* (6th Ed.). Saunders,Elsevier, pp. 474-631.

26. Thrall, D. E. 2018. *Text book of veterinary diagnostic radiology* (7th Ed.). Saunders,Elsevier, pp. 567- 733.

27. Virmani, R. 1995. Tumours metastatic to the heart and pericardium. In: Burke, A. and Virmani,

28. R. (eds.), *Atlas of tumour pathology. Tumours of the heart and great vessels.* (3rd Series) Fascicle, Washington, DC, pp.195–209.

29. Weerakkody and Niknejad 2019. Pulmonary Metastasis. Radiopaedia. Available: https://radiopaedia.org/articles/pulmonary-metastases. [On Dec 16].

30. Whitten, C.R., Khan, S., Munneke, G.J. and Grubnic, S. 2007. A diagnostic approach to mediastinal abnormalities. *Radiographics. 27:* 657-671.

31. Woodring, J.H. 1990. Pitfalls in the radiologic diagnosis of lung cancer. *AJR. Am J Roentgenol. 154:* 1165-1175.

32. Yildirim, F. and Gurel, A. 2012. Comparison between cytological and histopathological evaluations of canine mammary tumours. *Revue. Med. Vet. 163:* 116-122.

33. Yumuşak, N. and Kutsal, O. 2016. A comparative study between fine needle aspiration biopsy (FNAB) findings and histopathology in the evaluation of canine skin and skin adnexal tumors. *Ankara. Üniv. Vet Fak Derg. 63:* 393-400.